PUBLISHED ATTENUATION FUNCTIONS COMPARED TO 6/29/1992 LITTLE SKULL MOUNTAIN EARTHQUAKE MOTION

Renner B. Hofmann
Center for Nuclear Waste
Regulatory Analyses
6220 Culebra Road
San Antonio, Texas 78228
(210) 512-5308

Abou-Bakr K. Ibrahim
U.S. Nuclear Regulatory Commission
NMSS/DHLWM
OWFN 4 H3
Washington D.C. 20555-0001
(301) 504-2523

ABSTRACT

Several western U.S. strong motion acceleration earthquake attenuation functions are compared to peak accelerations recorded during the 6/29/1992 Little Skull Mountain, NV earthquake. The comparison revealed that there are several definitions of site-to-source distance and at least two definitions of peak acceleration in use. Probabilistic seismic hazard analysis (PSHA) codes typically predict accelerations assuming point sources. The computer code, SEISM 1, was developed for the eastern U.S. where ground motion attenuation is usually defined in terms of epicentral distance. Formulae whose distance definitions require knowledge of the earthquake fault slip zone dimensions may predict very different near-field accelerations when epicentral distance is used. Problems associated with this phenomenon and approximations to achieve more consistent PSHA results are derived.

I. INTRODUCTION

The Center for Nuclear Waste Regulatory Analyses (CNWRA) under direction of the Nuclear Regulatory Commission (NRC) Division of High Level Waste Management (DHLWM) has adapted the Lawrence Livermore National Laboratory (LLNL) PSHA code SEISM 1 (also called SHC[1]) to investigate the effects of alternative seismic and tectonic models of the Yucca Mountain region. The code was originally developed for the NRC Office of Nuclear Reactor Regulation (NRR) to evaluate eastern U.S. nuclear power plant seismic design criteria. Acceleration attenuation functions used in the eastern U.S. usually define site-to-source distance as epicentral distance and acceleration as the peak acceleration recorded on a horizontal seismograph component. As enhancement to SEISM 1, ground motion attenuation functions developed for the western U.S. were added to the program. These functions usually define site-to-source distance as the nearest distance to the fault rupture zone or to its projection on the earth's surface. One attenuation function uses hypocentral distance. Accelerations are often defined as the average of peak accelerations recorded on each of two horizontal seismograph components.

The occurrence of the M=5.6 6/29/1992 Little Skull Mountain earthquake provided an opportunity to compare observed ground motion[2] near Yucca Mountain, NV with published western U.S. attenuation functions[3,4,5,6]. **Figure** 1 depicts the preliminary epicenter and fault plane solution (the larger NE trending plane), and strong motion seismograph locations. Distances to the epicenter, fault slip plane (estimated from preliminary aftershock information) and hypocenter were determined.

Several empirical attenuation functions developed by Campbell[3], Joyner and Boore[5], and Atkinson[4] were investigated. Results from their formulae for M = 5.6 were compared with recent Little Skull Mountain earthquake accelerations. Schnabel and Seed's[6] M = 5.6 curve was compared directly. There are many other strong motion attenuation functions in the open literature[8,9]. SEISM 1 will also accept acceleration-spectra and pseudovelocity-spectra attenuation. However, for this study only the functions referenced above were incorporated in SEISM 1.

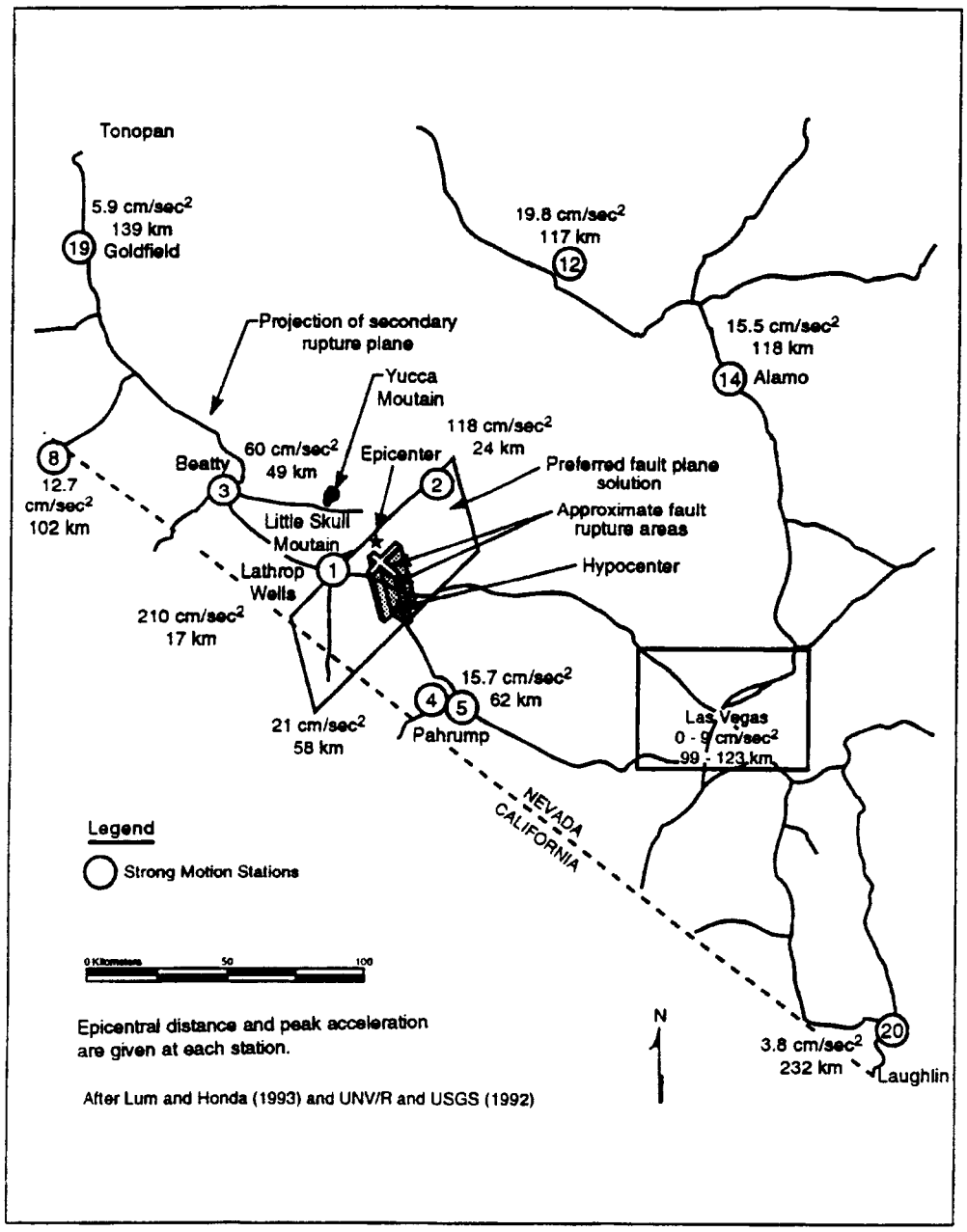

Figure 1. Strong Motion Seismographs and Fault Planes

II. ANALYSIS

Analysis of the preliminary Little Skull Mountain earthquake data was performed by first adjusting the attenuation formulae to a common definition of source-to-site distance and acceleration. Distance is defined as the shortest distance to the surface projection of the rupture plane. Acceleration is defined as the peak acceleration recorded on one of the horizontal seismograph components. A multiplication factor of 1.13 was used to derive peak from average-peak acceleration[3]. Preliminary analyses of the M=5.6 main shock and aftershocks provided a range of hypocentral depths. Values of 9[10] to 13km[7] were reported. An aftershock sequence plot[7] suggests a maximum slip plane depth of about 14 km. Aftershocks appear to define a rupture plane extending from 14 km to about 4 km of the surface, Figure 2. Other interpretations are possible. For this analysis, a depth of 14 km and a rupture plane extending to within 4 km of the surface were assumed. An estimate of along-strike (NE) rupture length of about 5.5 km is derived from the aftershock data of Figure 2.

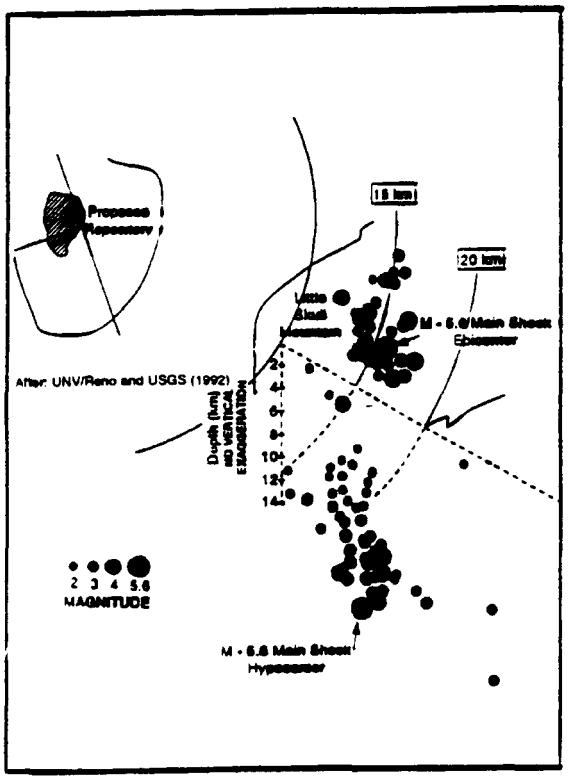

Figure 2. Little Skull Mountain Aftershocks

Using this assumed geometry, distances were converted to shortest distance to the surface projection of the rupture zone. In the case where distance is defined as hypocentral distance, epicentral distance was calculated assuming a 14 km depth of focus.

A. Strong Motion Data

Figure 1 contains the strong motion peak acceleration amplitudes and distances from published data[2]. For the stations closest to the source, closest distance to the rupture zone is calculated. The difference between this distance and epicentral distance is negligible for the more distant stations. These data are shown on Figure 3.

B. Fault Plane Solutions

Published fault plane solutions[7] from short-period near-field polarities and from the Harvard moment tensor solution, based on long period data, both indicate a normal fault striking NE-SW. Although both solutions indicate that the fault dips, they do not agree on the direction (NW or SE). See figure 1. The SE dip appears to be preferred[7].

C. Aftershock Data

An interpretation that two rupture planes are indicated by the aftershocks was published[11]. No illustration was provided but aftershock data suggests that the second plane is the NW trending one on Figure 1. These authors of this paper believe that the second, orthogonal, fault plane could also be a normal fault and the combined motion could be that of vertical movement of a block corner. This suggests near simultaneous rupture of the two faults which may explain the ambiguity in fault dip estimates. Figure 4 is a sketch of Landers fault movements derived from published data[7,12,13]. The sketched motions and reported geodetically determined displacements of 3 to 5 meters[13] or more suggest movement of a crustal block, possibly caused by the San Andreas fault being locked SE of the SE corner of the block surrounded by the Landis and Big Bear earthquake ruptures. The published Landers earthquake motions suggest that a diminution of stress in a direction toward Little Skull Mountain could be expected as a result. Whether the amount of stress could contribute to rupture at a distance of 280km is the subject of various opinions.

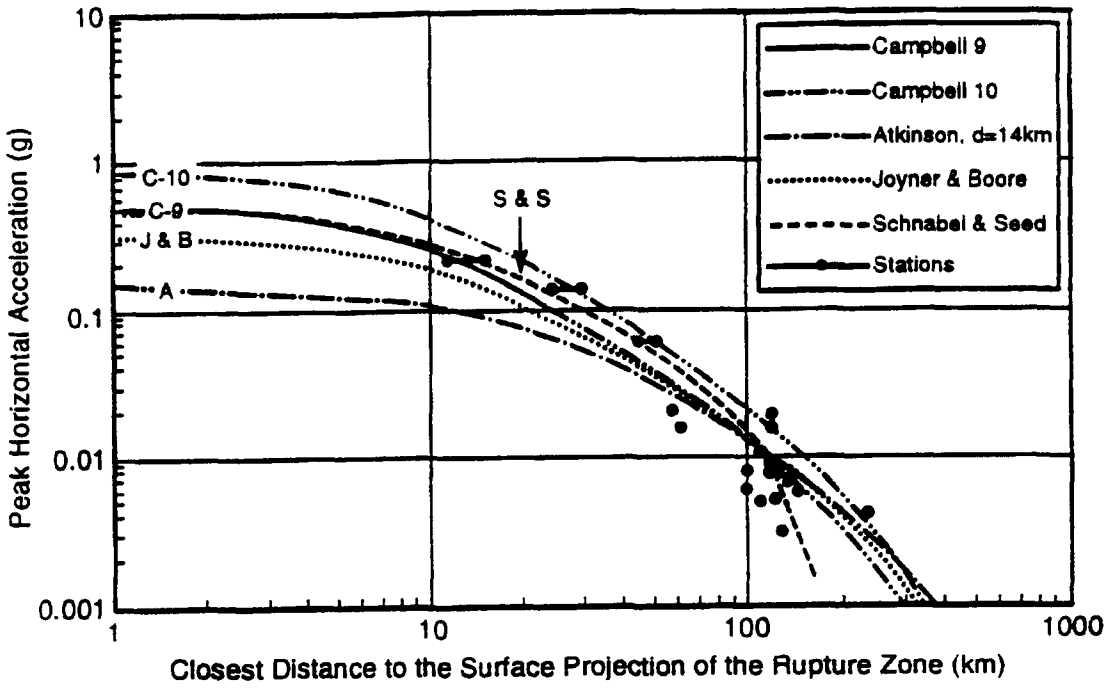

Figure 3. Modified Attenuation Functions for M=5.6

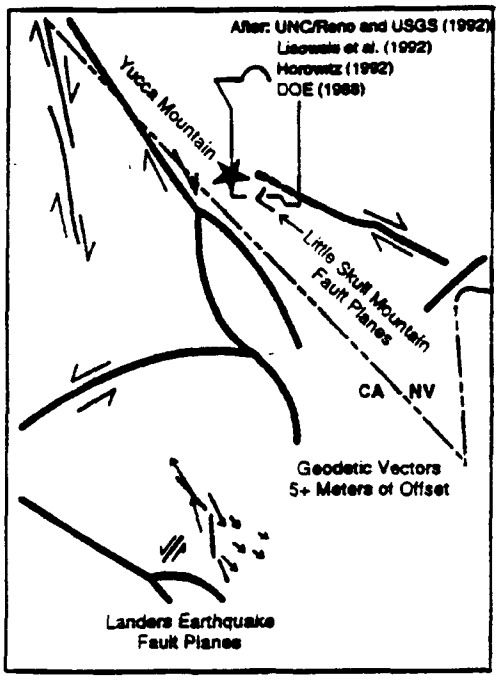

Figure 4. Landers Geodetic Vectors

One opinion holds that strain diminishes as the cube of distance and that therefore, strain at 100s of km from an earthquake source could not be perturbed by a large, distant earthquake[14]. Another view holds that for the Landers earthquake, succeeding not-too-distant fault ruptures were initiated which, in turn, triggered movement on another fault system etc. until large distances were influenced[15]. The point being made here, is that the direction of strain caused by the Landers earthquake would be favorable for normal faulting of a corner of a tectonic block bounded by two orthogonal faults, as may have occurred at Little Skull Mountain, assuming that the strain level at Yucca Mountain was non-negligible.

Aftershocks in **Figure 2** could be interpreted to represent a rupture plane which encompasses only the region of most closely spaced hypocenters or a larger one which encompasses all aftershock hypocenters. Distance to the surface projection of the rupture zone will change significantly for near-field stations depending on the rupture plane dimension chosen. Consequently, a range of distances is indicated on **Figure 3** for the three stations closest to the source. A relationship between magnitude and rupture area[16],

assuming a 100 bar stress drop, predicts about a 30 km^2 rupture area for a magnitude 5.6. The narrowest fault slip zone that could be interpreted from **Figure 2** would be about 4 km yielding a 40km^2 rupture area for the M=5.6 Little Skull Mountain earthquake. If the largest rupture width, encompassing most aftershocks, were chosen, the rupture area would be about 120 km^2. This would correspond to a magnitude of about 6.2 if stress drop is assumed to be an average of 100 bars. Some investigators[17] believe a lower stress drop, e.g. 36 bars may be appropriate for the Basin and Range tectonic province. In that case, the 120 km^2 area would be more appropriate. However, the 100 bar stress drop was originally established[17] primarily from California data. California also provide most of the empirical data from which strong motion attenuation functions are derived. In **Figures 3** and **5**, it can be seen that Little Skull Mountain strong motion data is higher than most of the magnitude 5.6 attenuation curves plotted, which suggests a higher stress drop than used in the derivation of the attenuation functions (whether by theory or empirically used earthquakes). Therefore, the smaller rupture area would appear to be more likely to be correct but considerable uncertainty remains.

ATTENUATION FUNCTIONS

The range of accelerations indicated on the three nearest stations to the Little Skull Mountain earthquake source on **Figures 3** represent epicentral distance on the right, and distance to the larger rupture area on the left. Distance to the smaller rupture area would be mid-range. **Figure 3** represents the selected attenuation functions with a common distance definition, closest-distance-to-the-surface-projection-of-the-rupture-zone. Acceleration is peak acceleration. Where the average of the peak acceleration recorded on each of two horizontal components is prescribed, the curve is multiplied by 1.13[3]. Atkinson's curve is plotted assuming a 14km hypocentral depth. If epicentral distance is used with the original attenuation functions on **Figure 5**, accelerations for the nearest Little Skull Mountain stations would not produce the author's intended result by a factor of about 1.8. For this attenuation function the value taken from **Figure 3**, would be too low. For longer faults and larger magnitudes, these differences could be larger. Acceleration differences caused by differences between epicentral and closest-to-the-rupture-zone distances would be accentuated on this log-log plot for still shorter distances. Data for the three nearest strong motion stations lie closest to the Schnabel and Seed[6] curve for peak acceleration on hard rock. If average peak acceleration from the two horizontal components is plotted against curves for average peak acceleration (not shown), Campbell's[3] curve for sediments less than 10 meters thick and restrained by far-field recordings, fits the data from the three nearest stations nearly as well. This suggests that converting curves from average peak to peak accelerations, or vice versa, by using a 1.13 factor may not do full justice to the original curve. Schnabel and Seed's curves were developed from peak acceleration data. Campbell's curves were developed from average-peak accelerations. If Atkinson's curves in **Figure 3** had not been adjusted from a 10 km depth of focus to a 14 km depth of focus, Little Skull Mountain earthquake data would be better represented by this curve. The author's original criteria would have produced better results than a formula modified to better represent the Little Skull Mountain preliminary depth of focus.

CONCLUSIONS

Distances as defined for various attenuation functions are shown to vary by as much as 50 percent for the near-field strong motion stations which recorded the Little Skull Mountain earthquake. Consequently, the published formulae were modified to better reflect distances to the Little Skull Mountain earthquake rupture zones as implied by aftershock data. However, adherence to the original formulae and presumed source conditions upon which they were based, would produce a somewhat better fit of the individual attenuation functions plotted, to the Little Skull Mountain strong motion data. Adjusting attenuation formulae to a common depth and distance definition improves accuracy over assuming epicentral distance and is computationally expedient. Slightly better results may be obtained by incorporating flexibility in the PSHA code to strictly adhere to the attenuation function's author's original definitions.

ACKNOWLEDGEMENTS

This effort was sponsored by the NRC. The views expressed are those of the authors and are not necessarily those of the NRC. Drs. H.L. McKague, K.I. McConnell and B. Sagar, and S.R. Young are respectfully acknowledged for their review and comments on this manuscript.

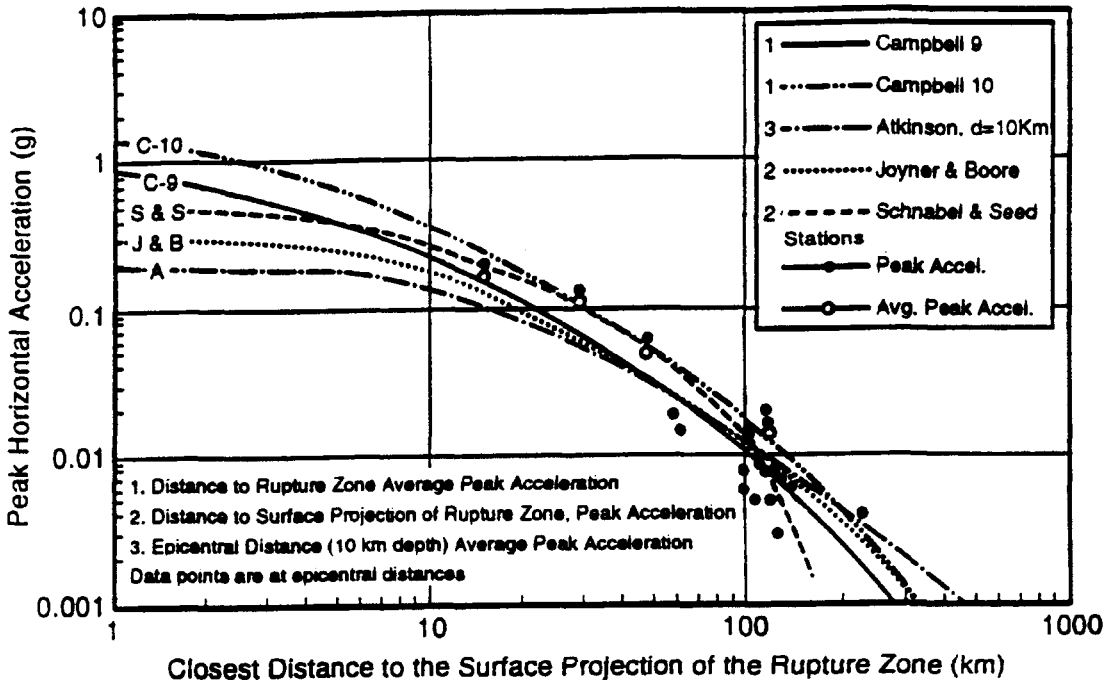

Figure 5. Original Accelerations Functions for M-5.6

NOMENCLATURE

Campbell 9	Campbell's[3] acceleration attenuation curve for sediments less than 10 meters thick constrained by far-field data.
Campbell 10	The Campbell 9 acceleration attenuation curve modified to include fault directivity for stations within 10 arc degrees of the fault strike.
CNWRA	Center for Nuclear Waste Regulatory Analyses
DHLWM	U.S. Nuclear Regulatory Commission Division of High Level Waste Management
DOE	U.S. Department of Energy
LLNL	Lawrence Livermore National Laboratory Richter magnitude defined as Richter local magnitude (ML) for magnitudes less than 6, 20 second surface wave magnitude (MS) for magnitudes from 6 to 8 and moment magnitude (M_W) for magnitudes greater than 8.
NRC	U.S. Nuclear Regulatory Commission
NRR	U.S. Nuclear Regulatory Commission Office of Nuclear Reactor Regulation
NV	Nevada
PSHA	Probabilistic seismic hazard analysis
SHC	Seismic Hazard Codes
USGS	U.S. Geological Survey
UNV/Reno	University of Nevada at Reno

REFERENCES

1. D. L. Bernreuter, J. B. Savy, R. W. Mensing, and D. H. Chung, *Seismic Hazard Characterization of the Eastern United States: Methodology and Interim Results for Ten Sites*, NUREG/CR-3756 U.S. Nuclear Regulatory Commission, Washington D.C. (1984).

2. P. K. Lum and K. K. Honda, *Processed Seismic Motion Records from Little Skull Mountain, Nevada Earthquake of June 29, 1992 Recorded at Stations in Southern Nevada*, URS/JAB-10733-TM6, UC-703 for the USDOE, URS/John A. Blume & Associates, Engineers, San Francisco, California (1993).

3. K. W. Campbell, "Predicting Strong Ground Motion in Utah", *Evaluation of Regional and Urban Earthquake Hazards and Risk in Utah*, W. W. Hays and P. L. Gori, editors, USGS Professional Paper 87-585II, pages L1-L90, U. S. Department of the Interior, Washington D.C. (1987).

4. G. M. Atkinson, "Attenuation of Strong Ground Motion in Canada from a Random Vibrations Approach", *Bulletin of the Seismological Society of America (BSSA)*, 74, 2629-2653 (1984).

5. W. B. Joyner and D. M. Boore, *Peak Horizontal Acceleration and Velocity from Strong Motion Records Including Records from the 1979 Imperial Valley Earthquake.* BSSA, 71, 2011-2038 (1981)

6. P. B. Schnabel and H. B. Seed, "Acceleration of Rock for Earthquakes in the Western United States", BSSA, 63, 501-516 (1973).

7. UNV/Reno & USGS, *The Little Skull Mountain Earthquake of June 29, 1992*, Letter Report of August 11, 1992 to the DOE, University of Nevada, Reno, Nevada (1992).

8. W. K. Campbell, "Strong Motion Attenuation Relations:A Ten Year Perspective", *Earthquake Spectra*, 1 365-376 (1985).

9. N. C. Donovan, "Strong Motion Attenuation Relations - A Critique", *Proceedings of the 3rd International Earthquake Microzonation Conference, Seattle, Washington*, 1 377-388 (1982).

10. DOE, *Reportable Geologic Condition*, Yucca Mountain Project Office (YMPO) report AP-6.14 (1992).

11. K. D. Smith, A. F. Sheehan, M. K. Savage, D. dePolo, J. N. Brune, and J. G. Aanderson, "Aftershocks of the June 29, 1992 M_L 5.6 Little Skull Mountain Earthquake" (abstract), *Seismological research Letters* 64 22 (1993).

12. F. G. Horowitz, "Minimum Energy Principle Obviates Stress buildup on San Andreas Associated with Mojave Event" (abstract), *EOS* Oct. 27, 358 (1992).

13. M. Lisowski, J. C. Savage, and W. K. Gross, "Geodolite and GPS measurements of Coseismic Deformation Near the Landers, California earthquake" (abstract), *(EOS)* Oct. 27, 358 (1992).

14. J. G. Anderson, J. Louie, J. N. Brune, D. dePolo, M. Savage, and G. Yu, "Seismicity in Nevada Apparently Triggered by the Landers,California Earthquake, June 28, 1992" (abstract, *EOS*, Oct. 27 392, (1992).

15. J. Gomberg and P. Bodin "Was the Little Skull Mountain Earthquake of June 29, 1992 Triggered by the Landers California Earthquake?" (abstract), *EOS* Oct. 27 392 (1992).

16. M. Wyss, "Estimating Maximum Expectable Magnitude of Earthquakes from Fault Dimensions", *Geology* 7 336-340 (1979).

17. C. L. Stark and W. J. Silva, "Assessment of Stress Drops of Normal-Faulting Earthquakes in the Basin and Range Province" (abstract), Seismological Research Letters 63 69 (1992).

18. DOE, "*Site Characterization Plan, Yucca Mountain Site Nevada Research and Development Area*", U.S. Department of Energy Office of Civilian Waste Radioactive Management, Washington D.C. (1988).